Journal of Ginseng Research 46 (2022) 700–709

Contents lists available at ScienceDirect

Journal of Ginseng Research

journal homepage: https://www.sciencedirect.com/journal/journal-of-ginseng-research

Research Article

Ginsenoside Rd protects cerebral endothelial cells from oxygen-glucose deprivation/reoxygenation induced pyroptosis via inhibiting SLC5A1 mediated sodium influx

Suping Li [a,1], Nengwei Yu [a,1], Fei Xu [a], Liang Yu [a], Qian Yu [b,**], Jing Fu [b,*]

[a] Department of Neurology, Sichuan Academy of Medical Sciences & Sichuan Provincial People's Hospital, Chengdu, China
[b] Department of Rehabilitation, Sichuan Academy of Medical Sciences & Sichuan Provincial People's Hospital, Chengdu, China

ARTICLE INFO

Article history:
Received 14 February 2022
Received in revised form
21 April 2022
Accepted 12 May 2022
Available online 21 May 2022

Keywords:
Ginsenoside Rd
HBMECs
NLRP3
Pyroptosis
SLC5A1

ABSTRACT

Background: Ginsenoside Rd is a natural compound with promising neuroprotective effects. However, the underlying mechanisms are still not well-understood. In this study, we explored whether ginsenoside Rd exerts protective effects on cerebral endothelial cells after oxygen-glucose deprivation/reoxygenation (OGD/R) treatment and its potential docking proteins related to the underlying regulations.
Method: Commercially available primary human brain microvessel endothelial cells (HBMECs) were used for *in vitro* OGD/R studies. Cell viability, pyroptosis-associated protein expression and tight junction protein degradation were evaluated. Molecular docking proteins were predicted. Subsequent surface plasmon resonance (SPR) technology was utilized for validation. Flow cytometry was performed to quantify caspase-1 positive and PI positive (caspase-1+/PI+) pyroptotic cells.
Results: Ginsenoside Rd treatment attenuated OGD/R-induced damage of blood-brain barrier (BBB) integrity *in vitro*. It suppressed NLRP3 inflammasome activation (increased expression of NLRP3, cleaved caspase-1, IL-1β and GSDMD-N terminal (NT)) and subsequent cellular pyroptosis (caspase-1+/PI + cells). Ginsenoside Rd interacted with SLC5A1 with a high affinity and reduced OGD/R-induced sodium influx and potassium efflux in HBMECs. Inhibiting SLC5A1 using phlorizin suppressed OGD/R-activated NLRP3 inflammasome and pyroptosis in HBMECs.
Conclusion: Ginsenoside Rd protects HBMECs from OGD/R-induced injury partially via binding to SLC5A1, reducing OGD/R-induced sodium influx and potassium efflux, thereby alleviating NLRP3 inflammasome activation and pyroptosis.

1. Introduction

Ginsenoside Rd is a key active component of Panax ginseng Meyer, which is also commonly found in Panax notoginseng, Panax quinquefolius and Gynostemma pentaphyllum [1]. Previous studies showed that it is a promising natural neuroprotective agent due to its anti-inflammative, anti-oxidative and anti-apoptotic regulations [1,2].

Ischemic stroke is a severe cerebrovascular disease associated with acute cerebral thrombosis. Tissue plasminogen activator (tPA) is the only therapeutic thrombolytic agent approved for acute ischemic stroke [3]. It induces the degradation of fibrin clots in a plasminogen-dependent manner. However, this agent only has a 4.5 h time window since the onset of ischemic stroke symptoms [3]. Another drawback is the increased risk of hemorrhage after reperfusion. This risk ranges from 2% to 7%, depending on the patient's own situation and the type of intracerebral hemorrhage [4]. This risk is largely caused by ischemia-reperfusion-induced cerebral vascular endothelial cell dysfunction, including damage to tight junctions, increased transcytosis, and a change to a pro-inflammatory phenotype [5].

The potential pre- and/or posttreatment effects of ginsenoside Rd on ischemic stroke-induced neural damages have been confirmed in previous studies [6–9]. In different experimental models, ginsenoside Rd could effectively reduce cortical neuron death, infarct volume, inflammation and improve cognitive and

* Corresponding author. Department of Neurology, Sichuan Academy of Medical Sciences & Sichuan Provincial People's Hospital, Chengdu, 610072, China.
** Corresponding author. Department of Rehabilitation, Sichuan Academy of Medical Sciences & Sichuan Provincial People's Hospital, Chengdu, 610072, China.
E-mail addresses: yqswc11@163.com (Q. Yu), 2091145921@qq.com (J. Fu).
[1] Suping Li and Nengwei Yu contributed equally to this study.

https://doi.org/10.1016/j.jgr.2022.05.006

neurological functions [2,10]. One recent study showed it prevents nicotine-induced cardiovascular disease by weakening the inflammatory status of normal vascular endothelial cells [11]. Mechanistically, it maintains normal NO signaling and reduces platelet aggregation, vasoconstriction, and monocyte adhesion [11]. However, only limited studies explored the effect of ginsenoside Rd on cerebral endothelial cells.

As a natural compound, ginsenoside Rd exerts protective effects through multiple signaling pathways [1,2]. Although there is convincing evidence supporting ginsenoside Rd's anti-inflammatory effects, the molecular mechanisms remain poorly understood. In this study, we explored whether ginsenoside Rd protects cerebral endothelial cells after oxygen-glucose deprivation/reoxygenation (OGD/R)-induced injury. Its potential docking proteins related to these regulations were also studied.

2. Materials and methods

2.1. Cell culture

Human brain microvessel endothelial cells (HBMECs) were obtained from Procell (CP—H124, Wuhan, China) and cultured using the recommended cultured medium (CM-H124, Procell) and conditions. Ginsenoside Rd (purity: 98.27%), MCC950 (a selective NLRP3 inflammasome inhibitor, purity: 99.7%) and phlorizin (a competitive inhibitor of SLC5A1 and SLC5A2, purity: 99.83%) were purchased from Selleck (Houston, TX, USA).

2.2. Oxygen-glucose deprivation/reoxygenation (OGD/R) treatment

When HBMECs reached 70–80% confluence, the cells were treated with ginsenoside Rd (5, 15 or 30 μM), phlorizin (25 or 50 μM) and MCC950 (1 μM) for 12 h. Then, the cells were washed and cultured in glucose-free culture medium in a hypoxic chamber (1% O_2, 5% CO_2 and 94% N_2) for 2 or 4 h. Afterward, cells were incubated for another 12 h under normoxia in complete medium. The same concentrations of drugs were also administered during the 12 h normoxic culture.

2.3. Trans-endothelial electrical resistance (TEER) assay

TEER assays [12] were performed with a Millicell ERS system equipped with chopstick electrodes (Millipore, Billerica, MA, USA). In brief, HBMECs were grown on the upper chamber of the 24-well transwell inserts (0.4 μm pores, Corning Incorporated, Corning, NY, USA) at a density of 2×10^5 cells in 0.5 ml medium. The same culture medium (1.5 ml) was added to the lower chamber. The TEER value was measured daily to identify the time of peak resistance and was reported as Ω/cm^2. The inserts with stabilized peak resistance were subjected to OGD/R, with or without indicating ginsenoside Rd treatment.

2.4. Assessment of paracellular permeability

The diffusion of FITC-dextran (70 kDa; Sigma-Aldrich, St. Louis, MO, USA) across the integrated monolayer was measured following the strategy introduced previously [13]. Briefly, the transwell inserts with HBMEC monolayer were firstly pretreated with ginsenoside Rd or phlorizin for 12 h and then subjected to OGD/R. After that, they were transferred into new wells filled with pre-warmed HBSS buffer for washing. FITC-dextran (1 mg/ml) was then added to the upper chamber and subjected to incubation at 37 °C for 60 min in the dark. Then, the samples in the lower chambers were transferred into a new black 96-well plate. Fluorescence intensity was measured using a fluorescence microplate reader (BioTek Synergy Neo 2, Agilent Technologies, Santa Clara, CA, USA) with excitation at 492 nm and emission at 518 nm. Relative fluorescence intensity was represented as fold-change.

2.5. Immunofluorescent staining

HBMECs cells grown on coverslips were cultured with 30 μM of ginsenoside Rd or 50 μM of phlorizin for 12 h. Then, cells were subjected to OGD(2 h)/R (12 h) treatment. Immunofluorescent staining was conducted following the methods described previously [14]. The coverslips were incubated with rabbit CoraLite594-Conjugated ZO-1 polyclonal antibody (1:200, CL594-21773, Proteintech, Wuhan, China) and mouse Alexa Fluor 488-Conjugated Claudin-5 monoclonal antibody (1:2000, 352,588, Thermo Fisher Scientific, Wortham, TX, USA) overnight at 4 °C. After washing with PBS, the coverslips were mounted using ProLong Gold Antifade Mountant with DAPI (Thermo Fisher Scientific). The fluorescence was examined with a confocal microcopy Olympus fluorescence FV1000 microscope.

2.6. Western blotting and cellular thermal shift assay (CETSA)

Western blotting was performed following the methods described previously [14]. Cultured HBMECs were harvested, washed, and lysed using RIPA lysis buffer with complete protease inhibitor cocktail (P0013B, Beyotime). The following primary antibodies were used: anti-ZO-1 (1:1000, #5406, Cell Signaling Technology, Danvers, MA, USA), anti-claudin-5 (1:1000, A10207, ABclonal, Wuhan, China), anti-NLRP3 (1:1000, A14223, ABclonal), anti-caspase-1 (1:1000, A0964, ABclonal), anti-IL-1β (1:1000, A16288, ABclonal), anti-Gasdermin D (GSDMD, #96458, 1:1000, Cell Signaling Technology), anti-SLC5A1 (1:1000, #5042, Cell Signaling Technology) and anti-SLC5A2 (1:1000, #14210, Cell Signaling Technology). The protein bands were developed using chemiluminescence detection reagents (BeyoECL Star, Beyotime, Shanghai, China). Protein expression was quantified by densitometry and normalized to β-actin using ImageJ software (version 1.37, NIH, Bethesda, MD, USA).

CETSA was conducted following the methods introduced previously [15]. 30 μM Ginsenoside Rd or vehicle control (DMSO) was incubated with the lysate supernatant collected above for 1 h at room temperature. Then, aliquots of the samples (50 μl) were treated with different temperatures (45, 55, 60, 65, and 70 °C) for 5 min, using a thermal cycler and cooled under room temperate for 5 min. Then, the samples were centrifuged (20,000 g for 20 min at 4 °C) again. The supernatants were subjected to western blotting assays using anti-SLC5A1 (1:1000, #5042, Cell Signaling Technology).

2.7. Flow cytometric analysis

The proportions of pyroptotic cells in each treatment group were measured by flow cytometry, following the method introduced previously [16]. In brief, Active caspase-1 was detected with FLICA 660 Caspase-1 Detection Kit (ImmunoChemistry, Davis, CA, USA). HBMECs were cultured in 6-well plates and subjected to indicated treatments. Then, cells were harvested and incubated with the FLICA 660 working solution (1:50, v/v). The cells were incubated at 37 °C for 45 min. Then, the cells were washed, centrifuged, resuspended, and stained with PI solution 5 min before analysis by a FACSCalibur flow cytometer (Becton, Dickinson and Company, San Diego, CA, USA).

2.8. Intracellular sodium and potassium ion levels

Changes in intracellular sodium and potassium levels were measured using fluorometric determination, using the fluorescent dye sodium-binding benzofuran isophthalate acetoxymethyl ester (SBFI-AM) and potassium-binding benzofuran isophthalate acetoxymethyl ester (PBFI-AM) as selective ion indicators respectively, following the method introduced previously [17]. In brief, after pretreatment with ginsenoside Rd or phlorizin, primary HBMECs were subjected to OGD(2 h)/R (1 h) treatment, with the presence of SBFI-AM or PBFI-AM (10 μM) and 0.05% pluronic F-127. Then, fluorescence intensities were measured using a fluorescent plate reader by setting excitation wavelengths at 344 nm and 400 nm and emission wavelength of 510 nm. Statistical analysis was performed by determining the ratio of the signals at 340 nm/380 nm, based on data from triple technical replicates for each independent experiment.

2.9. Prediction of ginsenoside Rd docking proteins

The potential ginsenoside Rd docking proteins were predicted using TargetNet (http://targetnet.scbdd.com/) [18]. In brief, the structure of ginsenoside Rd was transferred to Simplified Molecular Input Line Entry System (SMILES) chemical format for docking prediction. The predicted candidates with probability scores higher than 0.5 were identified. Then, the specific atomic interaction between ginsenoside Rd and SLC5A1 (https://alphafold.ebi.ac.uk/entry/P13866) was conducted using CB-Dock (http://clab.labshare.cn/cb-dock/php/index.php) [19]. Only the bound poses with Vina score lower than −5 were presented.

2.10. Surface plasmon resonance (SPR) analysis

The binding affinity of ginsenoside Rd to SLC5A1 protein was measured using a Biacore T200 (GE Healthcare, Pittsburgh, PA, USA). Human recombinant SLC5A1 protein (Novus Biologicals, Littleton, CO, USA) was captured on a CM5 chip via a standard amine coupling procedure. Binding sensorgrams were recorded by serially injecting diluted ginsenoside Rd over the immobilized SLC5A1 surface. Then, equilibrium dissociation constant (K_D) value was calculated with a steady affinity state model.

2.11. Real-time quantitative reverse transcription PCR (qRT-PCR)

qRT-PCR analysis was conducted as we described previously [14]. *SLC5A1* expression was normalized to that of *ACTB*, using the $2^{-\Delta\Delta CT}$ method. The following primers were used: *SLC5A1*, forward, 5′-CGCCTATCCAACCTTAGTGGTG-3′, reverse, 5′-CGCTGTTGAAGATGGAGGTCAG-3'; *ACTB*, forward, 5′-CACCATTGGCAATGAGCGGTTC-3′, reverse, 5′-AGGTCTTTGCGGATGTCCACGT-3'.

2.12. Statistical analysis

Data were integrated and analyzed using GraphPad Prism 8.01 software (GraphPad Software, San Diego, CA, USA). Multiple group comparison was conducted using one-way ANOVA test, followed by Tukey post hoc test. Welch's unpaired *t*-test was used for comparison between two groups. Results are expressed as mean ± standard derivation (SD). $p < 0.05$ was considered of significance.

3. Results

3.1. Ginsenoside Rd attenuates the OGD/R-induced damage of blood-brain barrier (BBB) integrity in vitro

The effect of ginsenoside Rd (10, 30 and 60 μM) (Fig. 1A) on the cell viability of HBMECs was assessed. Compared to the untreated control group, 60 μM ginsenoside Rd treatment for 24 h significantly reduced cell viability (100.7 ± 4.0% vs. 69.0 ± 4.6%, $p < 0.001$) (Fig. 1B). 30 μM ginsenoside Rd did not significantly alter the cell viability of HBMECs (Fig. 1B). Therefore, 30 μM was used as the maximal ginsenoside Rd concentration for *in vitro* studies.

HBMECs with or without pretreatment of ginsenoside Rd were subjected to OGD/R. OGD/R significantly impaired cell viability (Fig. 1C). However, 15 and 30 μM ginsenoside Rd significantly restored cell viability after OGD/R (Fig. 1C).

To explore whether ginsenoside Rd exerts protective effects on *in vitro* BBB integrity after OGD/R, HBMECs were cultured in transwell inserts under normoxia to form a monolayer (Fig. 1D). When the insert reached the peak TEER value, the cell monolayers with or without ginsenoside Rd pretreatment were subjected to OGD/R. Then, the TEER value was measured again. Results showed that OGD/R significantly decreased the TEER value of the HBMEC monolayer (Fig. 1E). Ginsenoside Rd showed a dose-dependent protective effect against the TEER drop in both OGD(2 h)/R (12 h) or OGD(4 h)/R (12 h) groups (Fig. 1E). The barrier protective effect was validated by FITC-dextran diffusion assays. The HBMEC monolayer with ginsenoside Rd treatment has a significantly lower permeability of FITC-dextran compared to the group without ginsenoside Rd treatment (Fig. 1F).

Tight junction proteins such as claudin-5, ZO-1 and occludin were important in maintaining the integrity of the BBB [20]. Immunofluorescent staining and western blotting confirmed showed that compared to the negative control (NC) group, OGD/R significantly reduced the protein content of ZO-1 and claudin-5 in HBMECs (Fig. 1G–J). However, ginsenoside Rd treatment reduced the loss of these two proteins (Fig. 1G–J).

3.2. Ginsenoside Rd suppresses OGD/R-activated NLRP3 inflammasome and pyroptosis in HBMECs

One recent study showed that OGD/R could activate NLRP3 inflammasome and pyroptosis in mouse brain-derived endothelial b.End 3 cells [21]. Therefore, we further tested whether ginsenoside Rd protects HBMECs from OGD/R-activated NLRP3 inflammasome and pyroptosis. OGD/R significantly increased the expression of NLRP3, cleaved caspase-1, IL-1β, and GSDMD-N terminal (NT) in HBMECs (Fig. 2A–E). Flow cytometric analysis showed that OGD/R significantly increased the ratio of pyroptotic cells (caspase-1+/PI + cells) (Fig. 2F–G). When cells were pretreated with ginsenoside Rd or MCC950 (1 μM), OGD/R-activated NLRP3 inflammasome and subsequent pyroptosis were significantly weakened (Fig. 2A–G).

3.3. Ginsenoside Rd binds to SLC5A1 with a high affinity

To explore the molecular mechanisms underlying the protective effects of ginsenoside Rd, we predicted its docking proteins using TargetNet [18]. Only the proteins with a probability score higher than 0.5 were identified as the candidates (Fig. 3A). Among the candidates, SLC5A1 (also called sodium-dependent glucose transporters 1, SGLT1) was significantly upregulated in cortical neurons and capillary endothelial cells after focal cerebral ischemia in the

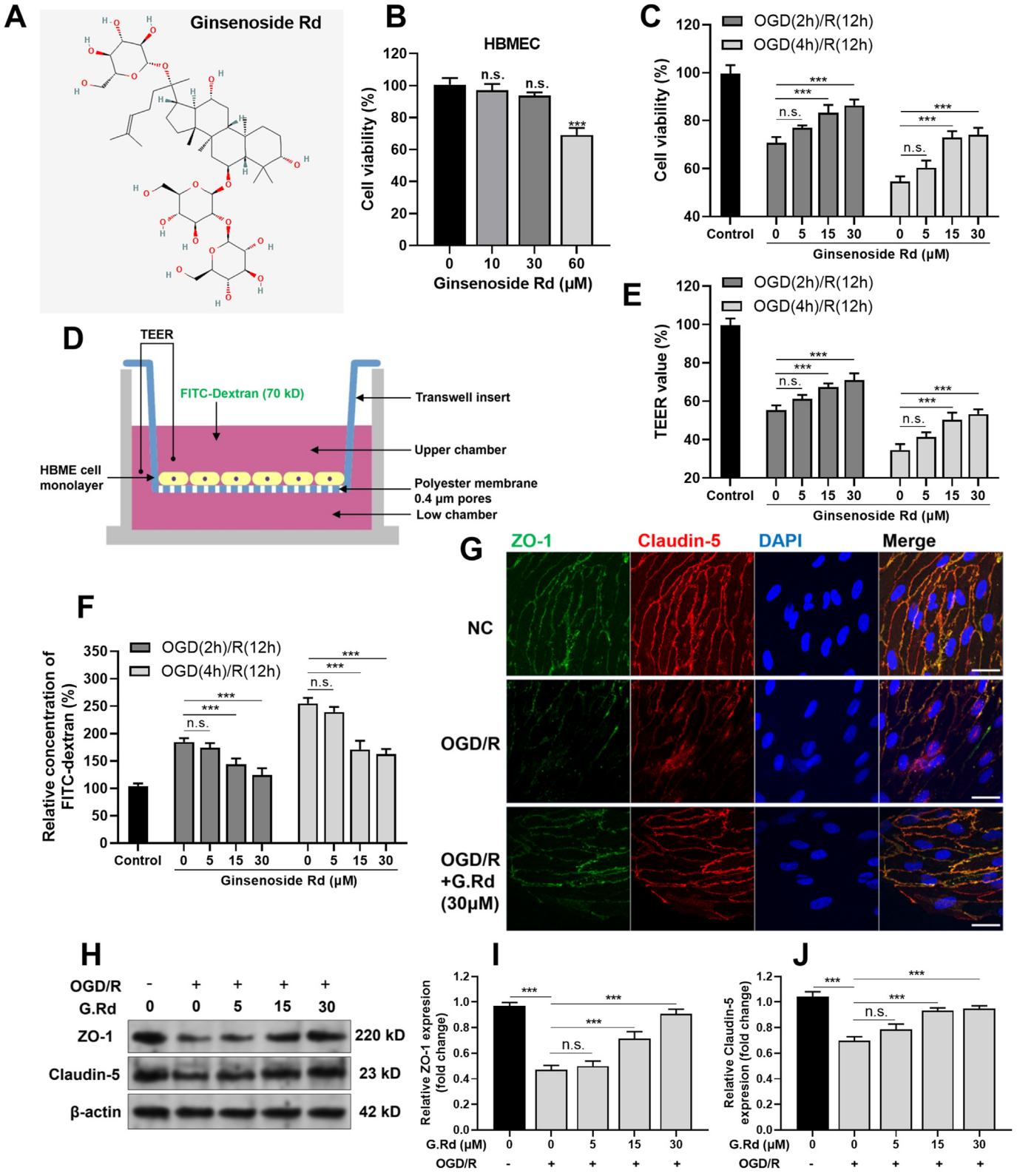

Fig. 1. Ginsenoside Rd attenuates the OGD/R-induced damage of blood-brain barrier (BBB) integrity *in vitro*. **A.** Chemical structure of ginsenoside Rd. **B.** Effect of ginsenoside Rd (10, 30, and 60 μM) treatment (24 h) on cell viability of HBMECs. **C.** CCK-8 assays were performed to assess the protective effects of ginsenoside Rd against OGD/R-induced loss of cell viability in different injury time. **D.** A schematic image of the *in vitro* BBB model. HBMECs were seeded on the top side of the transwell insert to form a monolayer. Then, TEER and paracellular diffusion of FITC-dextran (70 kDa) were measured. **E-F.** Relative TEER values (E) and relative concentration of FITC-dextran (F) were calculated to assess the protective effect of ginsenoside Rd (5, 15 and 30 μM) against OGD/R-induced damage of barrier function in different OGD/R time. **G-J.** Representative immunofluorescent images (G) and western blotting assays (H–J) showing the expression of ZO-1 (green) and claudin-5 (red) in HBMECs after OGD(2 h)/R (12 h), with or without treatment of ginsenoside Rd (30 μM). Scale bar = 20 μm. G.Rd: ginsenoside Rd. Results were reported as mean ± SD (n = 3). ***$p < 0.001$. n.s.: not significant.

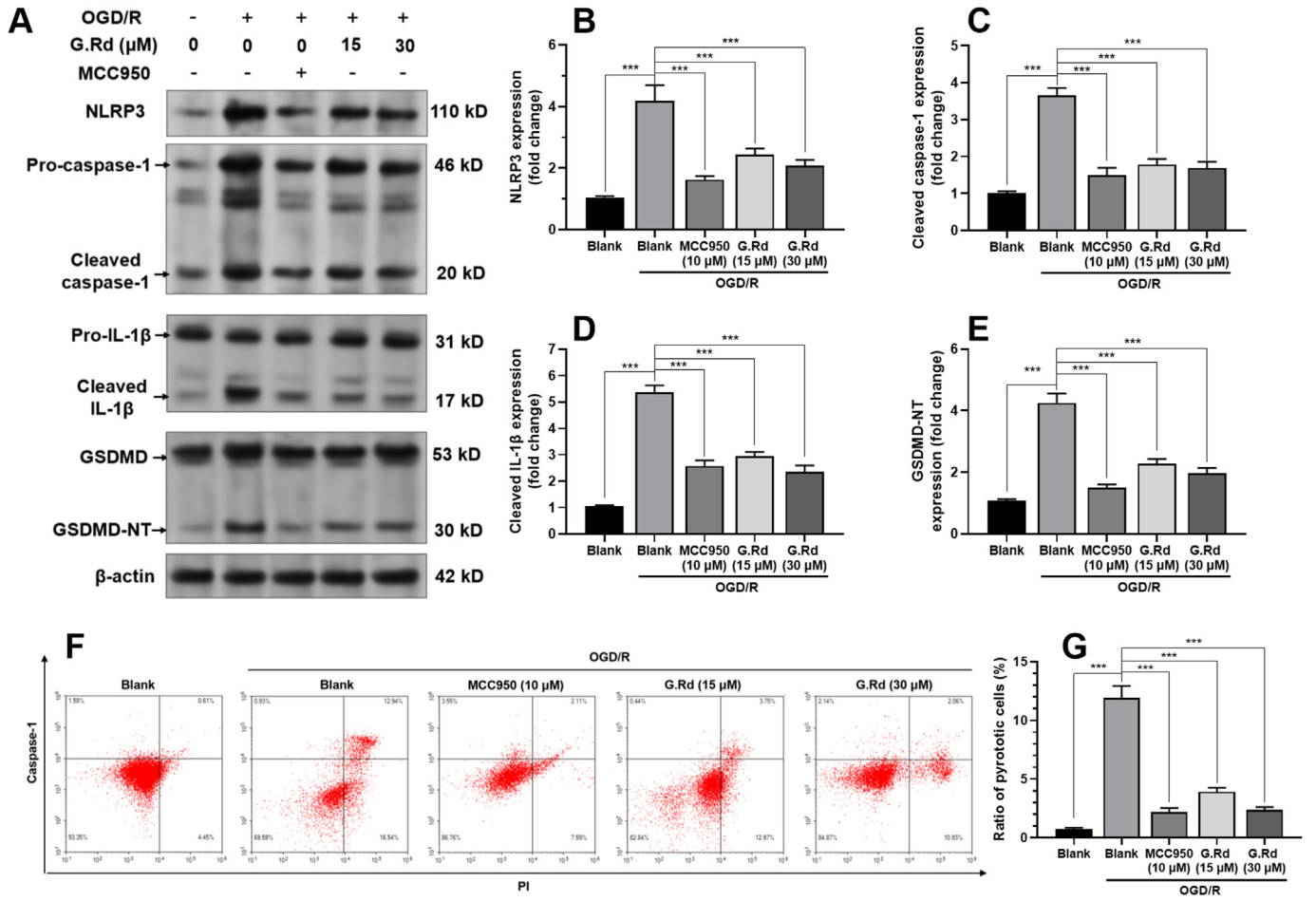

Fig. 2. Ginsenoside Rd suppressed OGD/R-activated NLRP3 inflammasome and pyroptosis in HBMECs. **A-E.** Representative blots (A) and quantitative analysis (B–E) of NLRP3, cleaved caspase-1, IL-1β and GSDMD-NT expression in HBMECs after OGD stimulation, with or without treatment of MCC950 (1 μM) or ginsenoside Rd (15 or 30 μM). **F-G.** Representative flow cytometric images (F) and quantitative data (G) of caspase-1+/PI + cell ratio were provided. Results were reported as mean ± SD (n = 3). ***$p < 0.001$. n.s.: not significant.

mouse and rat model of middle cerebral artery occlusion (MCAO) [22,23]. Its upregulation exacerbates neuronal damage caused by post-ischemic hyperglycemia [22,24]. Then, the potential interaction between ginsenoside Rd and the residuals of SLC5A1 was estimated by molecular docking, using CB-Dock [19]. Results showed that ginsenoside Rd has three high potential binding sites in SLC5A1, with dozens of binding residuals (Fig. 3B). Then, we checked the structural basis of SLC5A1 and the model of its interaction with glucose proposed by one previous study [25] (Fig. 3C). The sugar-binding site of SLC5A1 includes residues Q445, Q457, T460, R499, and Y506 (Fig. 3C, left). Residues on the external surface are highlighted in yellow blocks in the right panel (Fig. 3C, left). Therefore, ginsenoside Rd might directly bind to three critical glucose binding sites (Q445, R499 and E503) of SLC5A1 on its surface (Fig. 3B, red arrows). To confirm if ginsenoside Rd directly binds to SCL5A1, we utilized the SPR technology. Ginsenoside Rd exhibited a concentration-dependent binding with recombined human SLC5A1 protein, with an estimated K_D of 0.68 μM (Fig. 3D). Next, we conducted CETSA to check the melting curves of SLC5A1 generated in HBMEC lysates, with or without the presence of ginsenoside Rd. Results showed that compared to the DMSO group, 30 μM ginsenoside treatment increased the thermal stability of SLC5A1 (Fig. 3E–F). These results showed that ginsenoside Rd bind to SLC5A1 with a high affinity. Since it might bind to the critical glucose binding site, we hypothesized that ginsenoside Rd might interfere with the physiological functions of SLC5A1.

3.4. Ginsenoside Rd reduces OGD/R-induced sodium influx and potassium efflux in HBMECs

OGD/R resulted in significantly upregulated *SLC5A1* expression at the mRNA and protein levels (Fig. 4A–B). However, ginsenoside Rd treatment did not influence OGD/R-induced SLC5A1 upregulation (Fig. 4A–B). SLC5A1 mediates sodium-dependent glucose uptake [26]. Increased sodium influx after ischemic/reperfusion exacerbates cerebral neuronal damage [24]. Therefore, we monitored intracellular concentrations of Na^+ and K^+ after OGD/R and the potential influences of ginsenoside Rd. Results showed that OGD/R significantly elevated intracellular Na^+ concentration but lower intracellular K^+ concentration (Fig. 4C–D). These alterations were significantly alleviated by ginsenoside Rd and phlorizin (a SLC5A1/SLC5A2 inhibitor and Na+/K + -ATPase inhibitor) treatment (Fig. 4C–D). Similar to ginsenoside Rd, phlorizin treatment showed protective effects on OGD/R-induced damage to *in vitro* BBB integrity (Fig. 4E–F) and the loss of tight junction proteins (Fig. 4G–J).

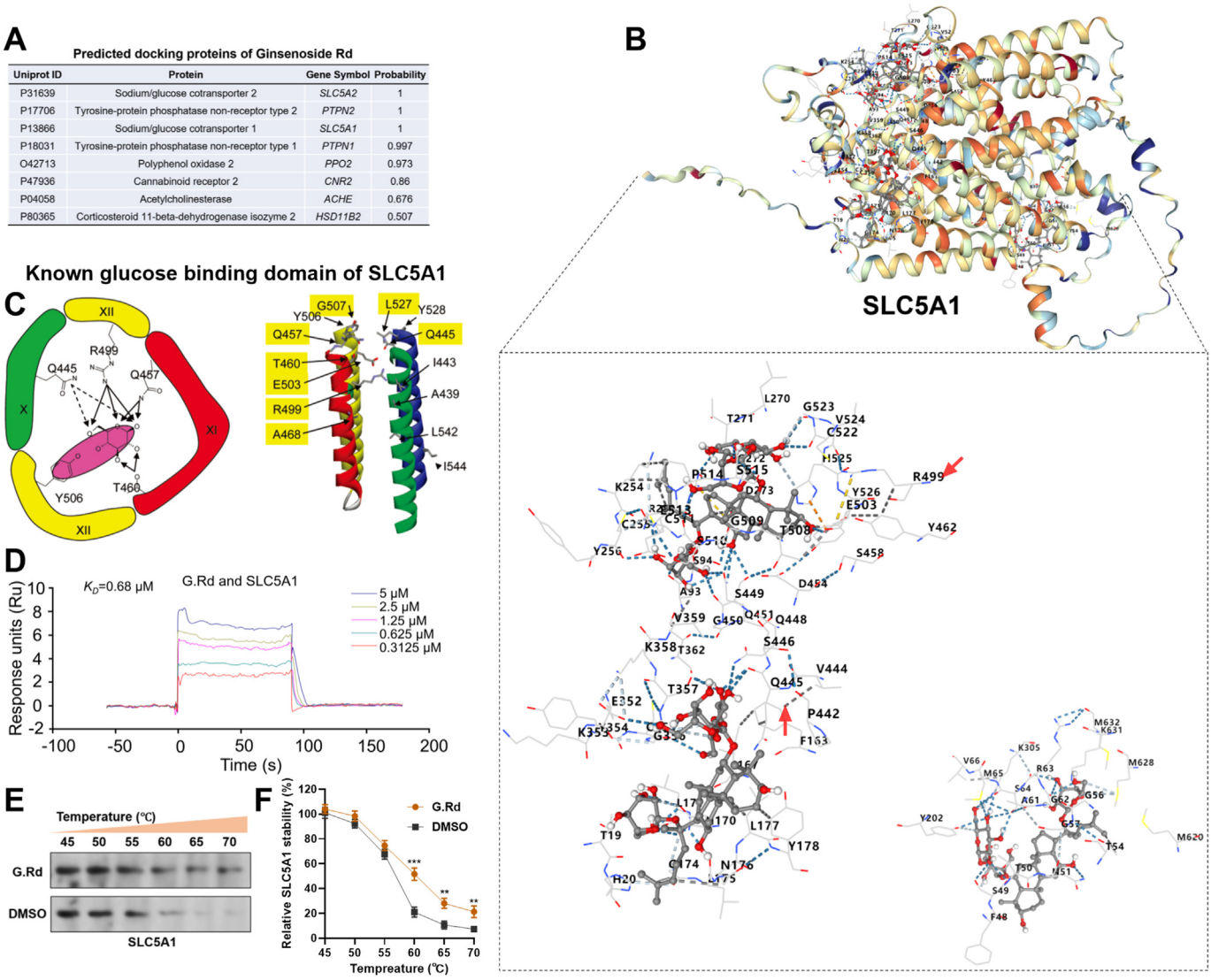

Fig. 3. Ginsenoside Rd binds to SLC5A1 with a high affinity. **A.** Predicted docking protein of ginsenoside Rd, by using TargetNet. **B.** Molecular docking of between ginsenoside Rd and SLC5A1. The estimated thee binding positions and related residuals within SLC5A1 were provided in the bottom panel. **C.** Left: schematic of proposed interactions between SLC5A1 and glucose by one previous study [25]. X, XI, XII and XIII are four translocation domains of SLC5A1. The magenta ellipse indicates the aromatic stacking with the hydrophobic surface of the pyranose. Right: Three-dimensional model of the glucose binding domains of SLC5A1 [25]. The same helical domains in the left and right panels are labeled with the same color. Residues on the external surface are highlighted with yellow boxes in the right panel. **D.** SPR analysis of ginsenoside Rd binding to human recombinant SLC5A1 protein. **E-F.** Representative images (E) and quantitation (F) of CETSA of SLC5A1 with 30 μM ginsenoside Rd. n = 3 independent experiments. $^{**}p < 0.01$, $^{***}p < 0.001$.

3.5. Inhibiting SLC5A1 suppresses OGD/R-activated NLRP3 inflammasome and pyroptosis in HBMECs

Therefore, we checked whether inhibiting SLC5A1 alleviates OGD/R-activated NLRP3 inflammasome and pyroptosis. HBMECs pretreated with phlorizin had reduced expression of NLRP3, cleaved caspase-1, IL-1β and GSDMD-NT (Fig. 5A–E), and a lower ratio of pyroptosis (caspase-1+/PI + cells) (Fig. 5F–G).

4. Discussion

Although natural protopanaxadiol ginsenosides exhibit low absorption in the human intestine, recent human pharmacokinetic studies following administration of red ginseng extract suggested that ginsenoside Rd is detected in the human plasma samples [27,28]. Therefore, although there might be no active absorption, there is still intestinal permeability of Rd, with slow elimination [28]. Similar findings were observed in mice and rats following the repeated oral administration of red ginseng extract [29]. Ginsenoside Rd has been characterized as a promising natural compound with neuroprotective effects and a potential clinical candidate drug for treating neurological diseases [1,10]. However, the molecular mechanisms supporting its neuroprotective effects remain fully illustrated. In the murine stroke model, NLPR3 inflammasome inhibition alleviates hypoxic endothelial cell death and helps maintain the BBB integrity [30]. The NLPR3 inflammasome-inhibiting effects of ginsenoside Rd were observed in mice model of colitis [31] and microglia cells in mice model of ischemia brain injury [8]. Therefore, we focused on the effect of ginsenoside Rd on NLPR3 inflammasome activation and the following pyroptosis in human microvessel endothelial cells. Using HBMECs as *in vitro* cell model, we explored the effect of ginsenoside Rd on OGD/R-induced endothelial cell injury. Our findings demonstrated that ginsenoside Rd treatment attenuated OGD/R-induced damage of BBB

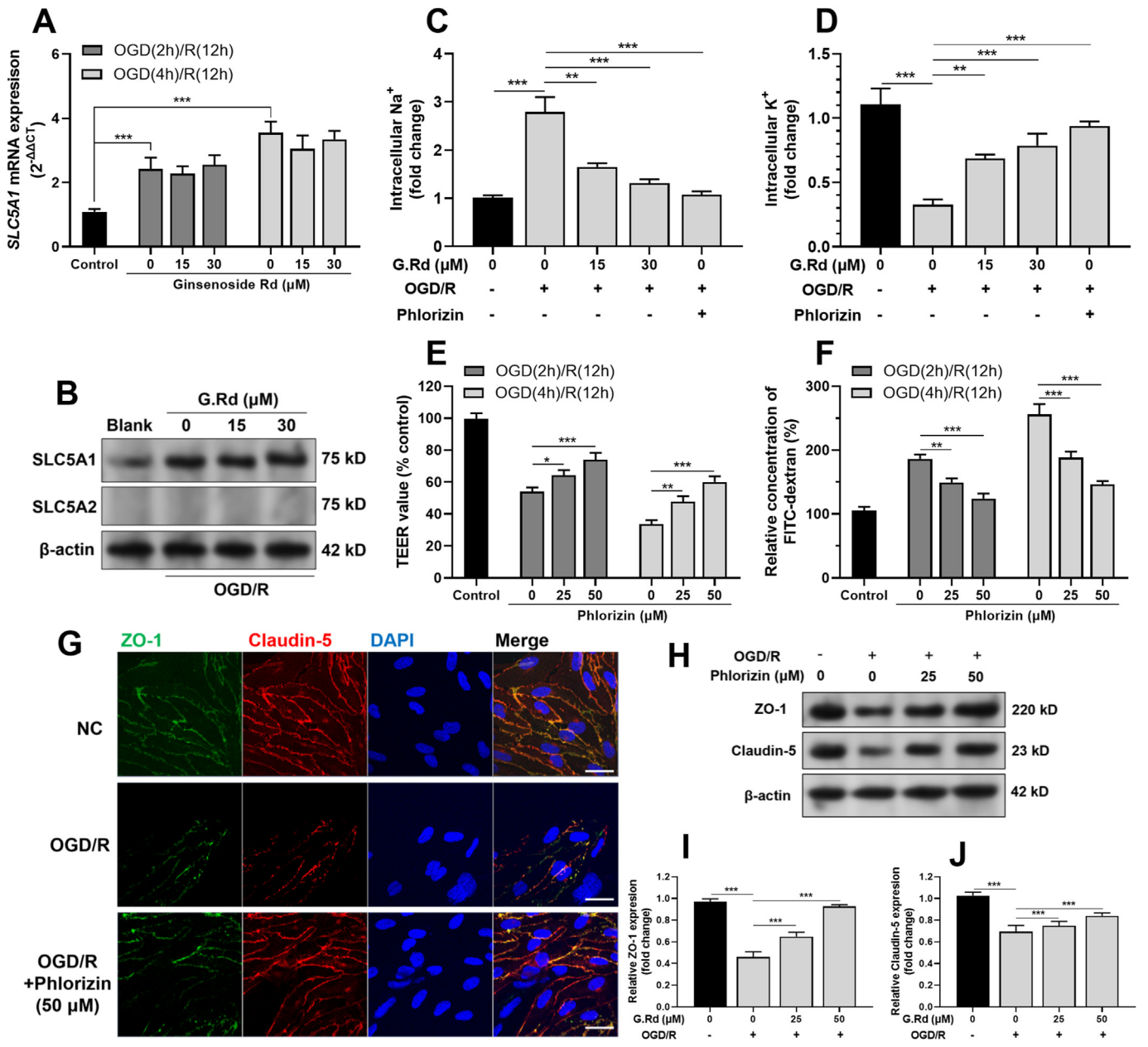

Fig. 4. Ginsenoside Rd reduces OGD/R-induced sodium influx and potassium efflux in HBMECs. **A.** *SLC5A1* mRNA expression in HBMECs after OGD/R stimulation, with or without treatment of ginsenoside Rd. **B.** SLC5A1 and SLC5A2 protein expression in HBMECs after OGD/R stimulation, with or without treatment of ginsenoside Rd. **C-D.** Relative intracellular Na^+ (C) and K^+ (D) were detected in HBMECs after OGD(2 h)/R (1 h) stimulation, with or without the presence of ginsenoside Rd. **E-F.** Relative TEER values (E) and relative concentration of FITC-dextran (F) were calculated to assess the protective effect of phlorizin (25 and 50 μM) against OGD/R-induced damage of barrier function in different OGD/R time. **G-J.** Representative immunofluorescent images (G) and western blotting assays (H–J) showing the expression of ZO-1 (green) and claudin-5 (red) in HBMECs after OGD(2 h)/R (12 h), with or without phlorizin treatment (50 μM). Scale bar = 20 μm. Results were reported as mean ± SD (n = 3). ***$p < 0.001$. n.s.: not significant.

integrity *in vitro* and the loss of tight-junction proteins (ZO-1 and Claudin-5). Claudin-5 is the most enriched tight junction protein in the BBB and acts as a gatekeeper of neurological function [32]. In addition, ginsenoside Rd suppressed NLRP3 inflammasome activation and subsequent cellular pyroptosis.

As a natural compound, the regulative effects of ginsenoside Rd might largely rely on its docking proteins. It binds to the epidermal growth factor receptor (EGFR) with a high binding affinity and inhibits the metastasis of colorectal cancer [33]. It inhibits hepatic uptake of phiopogonin D by organic anion-transporting polypeptides [34]. It blocks the activity of calcineurin, a key phosphatase for activating Death Associated Protein Kinase 1 (DAPK1), thereby inhibiting NMDA receptor (NMDAR)-triggered currents and sequential excitotoxicity [35]. By bioinformatic molecular docking and subsequent SPR analysis, we revealed that ginsenoside Rd interacts with SLC5A1 with a high affinity. Both SLC5A1 and SLC5A2 are important mediators of epithelial glucose transporters. SLC5A2 is almost exclusively expressed in the kidney and is responsible for glucose reabsorption from the tubular system, while SLC5A1 mediates glucose absorption in the small intestine [36]. In addition, SLC5A1 is also expressed in the skeletal muscles, heart and brain [37]. Based on five eligible randomized clinical trials (EMPA-REG (Empagliflozin), CANVAS (Canagliflozin), DECLARE-TIMI 58 (Dapagliflozin), CREDENCE (Canagliflozin) and

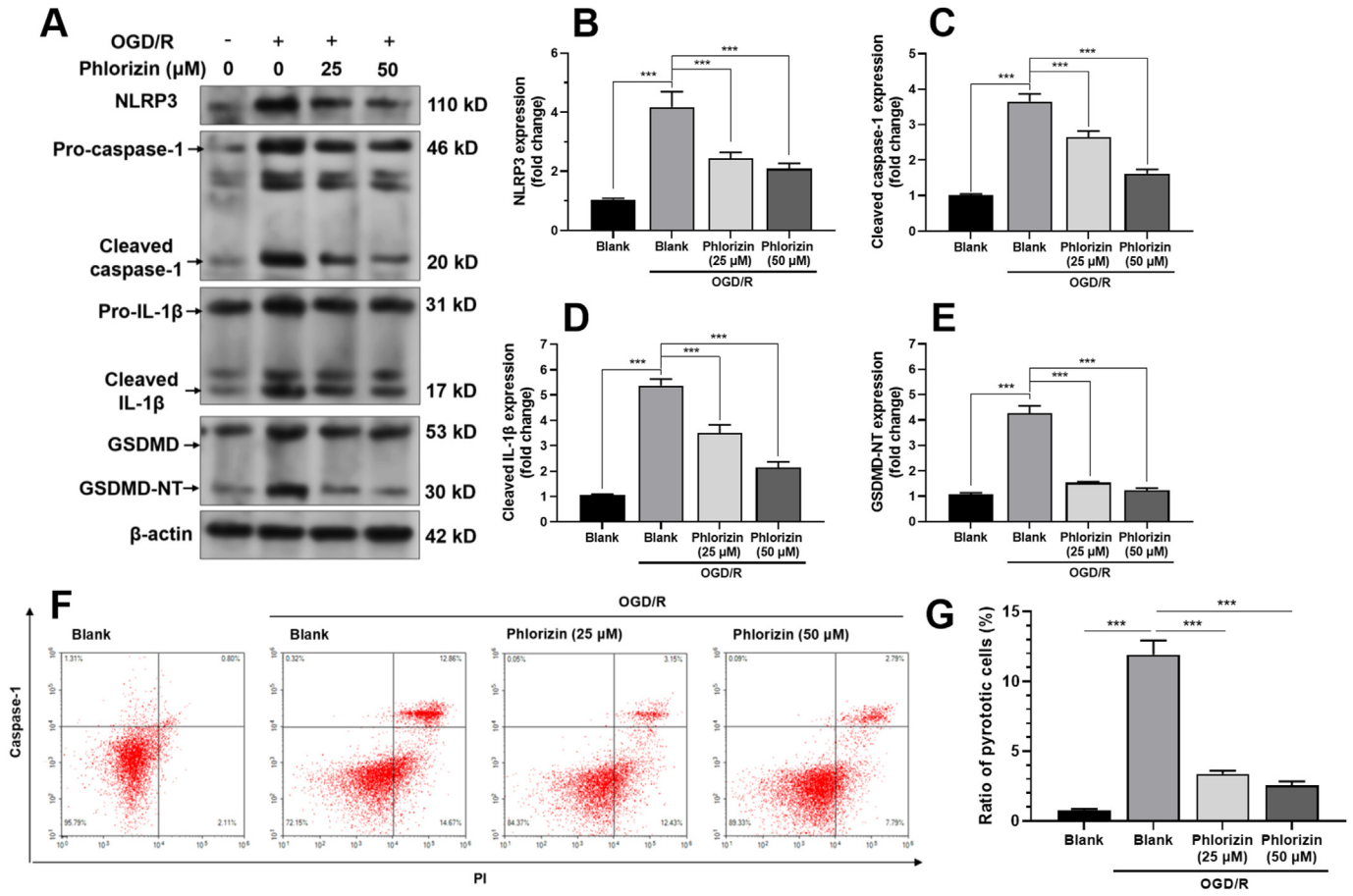

Fig. 5. Inhibiting SLC5A1 suppresses OGD/R-activated NLRP3 inflammasome and pyroptosis in HBMECs. **A-E.** Representative blots (A) and quantitative analysis (B–E) of NLRP3, cleaved caspase-1, IL-1β and GSDMD-NT expression in HBMECs after OGD stimulation, with or without phlorizin treatment. **F-G.** Pyroptotic cells with the same treatment in panel A were assessed by caspase-1 and PI staining. Representative flow cytometric images (F) and quantitative data (G) of caspase-1+/PI + cell ratio were provided. Results were reported as mean ± SD (n = 3). ***$p < 0.001$.

VERTIS CV (Ertugliflozin)) involving 46,969 participants, SLC5A2 inhibitors were associated with a significant 50% reduction of hemorrhagic stroke risk [38]. Although these SLC5A2 inhibitors had higher affinities to SLC5A2 compared to SLC5A1, they still bind to SLC5A1 [39]. Therefore, SLC5A inhibitors might have potential microvascular protective effects.

SLC5A1 mediates sodium-dependent glucose uptake and transports two Na^+ ions with one D-glucose molecule against the concentration gradients [26]. Its upregulation was observed in rat cerebral endothelial cells after OGD/R [23,40] and was confirmed in HBMECs in the current study. Ginsenoside Rd could not alter *SCL5A1* expression. In the current studies, we confirmed that HBMECs had significantly elevated intracellular Na^+ concentration and decreased K^+ concentration. Ginsenoside Rd treatment significantly reversed these alterations. Previous studies showed that K^+ efflux is a common activator of NLRP3 inflammasome activation, which is required and adequate for caspase-1 activation [41]. Besides, sodium influx exacerbates NLRP3-dependent inflammation [17]. Therefore, we infer that via binding to SLC5A1, ginsenoside Rd could reduce OGD/R-induced sodium influx and potassium efflux in HBMECs. Using phlorizin as a positive control of SLC5A1 selective inhibitor, we confirmed that by SLC5A1 inhibition could weaken OGD/R-induced damage to *in vitro* BBB integrity and alleviate OGD/R-activated NLRP3 inflammasome and pyroptosis of HBMECs.

Compared to ginsenoside Rd, the metabolite compound K has a significantly higher diffusion rate and area under the plasma drug concentration-time curve (AUC) [27,28]. Our preliminary studies showed that compound K still binds to SLC5A1, with similar binding sites with ginsenoside Rd (data were not shown here). Therefore, it is meaningful to further assess the functional role in compound K in *in vivo* studies.

Conclusion

This study revealed a novel mechanism of ginsenoside Rd in protecting HBMECs from OGD/R-induced injury. It binds to SLC5A1 with a high affinity and reduces OGD/R-induced sodium influx and potassium efflux, thereby alleviating NLRP3 inflammasome activation and pyroptosis of HBMECs. However, animal studies are supposed to be performed to validate these molecular mechanisms *in vivo*.

Funding

This study was supported by the Key Research Project of the Science & Technology Department of Sichuan Province, China (2021YFS0131 and 2020YFS0414).

Acknowledgment

The authors have no conflict of interest.

References

[1] Chen YY, Liu QP, An P, Jia M, Luan X, Tang JY, et al. Ginsenoside Rd: a promising natural neuroprotective agent. Phytomedicine 2022;95:153883. https://doi.org/10.1016/j.phymed.2021.153883. Epub 2021/12/25PubMed PMID: 34952508.

[2] Ye R, Zhao G, Liu X. Ginsenoside Rd for acute ischemic stroke: translating from bench to bedside. Expert Rev Neurother 2013;13(6):603–13. https://doi.org/10.1586/ern.13.51. Epub 2013/06/07PubMed PMID: 23738998.

[3] Hurd MD, Goel I, Sakai Y, Teramura Y. Current status of ischemic stroke treatment: from thrombolysis to potential regenerative medicine. Regen Ther 2021;18:408–17. https://doi.org/10.1016/j.reth.2021.09.009. Epub 2021/11/02PubMed PMID: 34722837; PubMed Central PMCID: PMCPMC8517544.

[4] Yaghi S, Willey JZ, Cucchiara B, Goldstein JN, Gonzales NR, Khatri P, et al. Treatment and outcome of hemorrhagic transformation after intravenous alteplase in acute ischemic stroke: a scientific statement for Healthcare professionals from the American heart association/American stroke association. Stroke 2017;48(12):e343–61. https://doi.org/10.1161/STR.0000000000000152. Epub 2017/11/04PubMed PMID: 29097489.

[5] Andjelkovic AV, Xiang J, Stamatovic SM, Hua Y, Xi G, Wang MM, et al. Endothelial targets in stroke: translating animal models to human. Arterioscler Thromb Vasc Biol 2019;39(11):2240–7. https://doi.org/10.1161/ATVBAHA.119.312816. Epub 2019/09/13PubMed PMID: 31510792; PubMed Central PMCID: PMCPMC6812626.

[6] Zhang X, Shi M, Bjoras M, Wang W, Zhang G, Han J, et al. Ginsenoside Rd promotes glutamate clearance by up-regulating glial glutamate transporter GLT-1 via PI3K/AKT and ERK1/2 pathways. Front Pharmacol 2013;4:152. https://doi.org/10.3389/fphar.2013.00152. Epub 2014/01/01PubMed PMID: 24376419; PubMed Central PMCID: PMCPMC3858668.

[7] Hu G, Wu Z, Yang F, Zhao H, Liu X, Deng Y, et al. Ginsenoside Rd blocks AIF mitochondrio-nuclear translocation and NF-kappaB nuclear accumulation by inhibiting poly(ADP-ribose) polymerase-1 after focal cerebral ischemia in rats. Neurol Sci 2013;34(12):2101–6. https://doi.org/10.1007/s10072-013-1344-6. Epub 2013/03/07PubMed PMID: 23463404.

[8] Hu J, Zeng C, Wei J, Duan F, Liu S, Zhao Y, et al. The combination of Panax ginseng and Angelica sinensis alleviates ischemia brain injury by suppressing NLRP3 inflammasome activation and microglial pyroptosis. Phytomedicine 2020;76:153251. https://doi.org/10.1016/j.phymed.2020.153251. Epub 2020/06/13PubMed PMID: 32531700.

[9] Ye R, Zhang X, Kong X, Han J, Yang Q, Zhang Y, et al. Ginsenoside Rd attenuates mitochondrial dysfunction and sequential apoptosis after transient focal ischemia. Neuroscience 2011;178:169–80. https://doi.org/10.1016/j.neuroscience.2011.01.007. Epub 2011/01/12PubMed PMID: 21219973.

[10] Nabavi SF, Sureda A, Habtemariam S, Nabavi SM. Ginsenoside Rd and ischemic stroke; a short review of literatures. J Ginseng Res 2015;39(4):299–303. https://doi.org/10.1016/j.jgr.2015.02.002. Epub 2016/02/13PubMed PMID: 26869821; PubMed Central PMCID: PMCPMC4593783.

[11] Zhang B, Hu X, Wang H, Wang R, Sun Z, Tan X, et al. Effects of a dammarane-type saponin, ginsenoside Rd, in nicotine-induced vascular endothelial injury. Phytomedicine 2020;79:153325. https://doi.org/10.1016/j.phymed.2020.153325. Epub 2020/09/14PubMed PMID: 32920289.

[12] Srinivasan B, Kolli AR, Esch MB, Abaci HE, Shuler ML, Hickman JJ. TEER measurement techniques for in vitro barrier model systems. J Lab Autom 2015;20(2):107–26. https://doi.org/10.1177/2211068214561025. Epub 2015/01/15PubMed PMID: 25586998; PubMed Central PMCID: PMCPMC4652793.

[13] Hu S, Wu Y, Zhao B, Hu H, Zhu B, Sun Z, et al. Panax notoginseng saponins protect cerebral microvascular endothelial cells against oxygen-glucose deprivation/reperfusion-induced barrier dysfunction via activation of PI3K/Akt/Nrf 2 antioxidant signaling pathway. Molecules 2018;23(11). https://doi.org/10.3390/molecules23112781. Epub 2018/10/31PubMed PMID: 30373188; PubMed Central PMCID: PMCPMC6278530.

[14] Li S, Fu J, Wang Y, Hu C, Xu F. LncRNA MIAT enhances cerebral ischaemia/reperfusion injury in rat model via interacting with EGLN2 and reduces its ubiquitin-mediated degradation. J Cell Mol Med 2021;25(21):10140–51. https://doi.org/10.1111/jcmm.16950. Epub 2021/10/24PubMed PMID: 34687132; PubMed Central PMCID: PMCPMC8572800.

[15] Peng Y, Zhang X, Zhang T, Grace PM, Li H, Wang Y, et al. Lovastatin inhibits Toll-like receptor 4 signaling in microglia by targeting its co-receptor myeloid differentiation protein 2 and attenuates neuropathic pain. Brain Behav Immun 2019;82:432–44. https://doi.org/10.1016/j.bbi.2019.09.013. Epub 2019/09/23PubMed PMID: 31542403.

[16] Li H, Jiang W, Ye S, Zhou M, Liu C, Yang X, et al. P2Y14 receptor has a critical role in acute gouty arthritis by regulating pyroptosis of macrophages. Cell Death Dis 2020;11(5):394. https://doi.org/10.1038/s41419-020-2609-7. Epub 2020/05/28PubMed PMID: 32457291; PubMed Central PMCID: PMCPMC7250907.

[17] Scambler T, Jarosz-Griffiths HH, Lara-Reyna S, Pathak S, Wong C, Holbrook J, et al. ENaC-mediated sodium influx exacerbates NLRP3-dependent inflammation in cystic fibrosis. Elife 2019;8. https://doi.org/10.7554/eLife.49248. Epub 2019/09/19PubMed PMID: 31532390; PubMed Central PMCID: PMCPMC6764826.

[18] Yao ZJ, Dong J, Che YJ, Zhu MF, Wen M, Wang NN, et al. TargetNet: a web service for predicting potential drug-target interaction profiling via multi-target SAR models. J Comput Aided Mol Des 2016;30(5):413–24. https://doi.org/10.1007/s10822-016-9915-2. Epub 2016/05/12PubMed PMID: 27167132.

[19] Liu Y, Grimm M, Dai WT, Hou MC, Xiao ZX, Cao Y. Cb-Dock: A web server for cavity detection-guided protein-ligand blind docking. Acta Pharmacol Sin 2020;41(1):138–44. https://doi.org/10.1038/s41401-019-0228-6. Epub 2019/07/03PubMed PMID: 31263275; PubMed Central PMCID: PMCPMC7471403.

[20] Lv J, Hu W, Yang Z, Li T, Jiang S, Ma Z, et al. Focusing on claudin-5: a promising candidate in the regulation of BBB to treat ischemic stroke. Prog Neurobiol 2018;161:79–96. https://doi.org/10.1016/j.pneurobio.2017.12.001. Epub 2017/12/09PubMed PMID: 29217457.

[21] Wang Y, Guan X, Gao CL, Ruan W, Zhao S, Kai G, et al. Medioresinol as a novel PGC-1 alpha activator prevents pyroptosis of endothelial cells in ischemic stroke through PPARalpha-GOT1 axis. Pharmacol Res 2021;169:105640. https://doi.org/10.1016/j.phrs.2021.105640. Epub 2021/04/30PubMed PMID: 33915296.

[22] Yamazaki Y, Ogihara S, Harada S, Tokuyama S. Activation of cerebral sodium-glucose transporter type 1 function mediated by post-ischemic hyperglycemia exacerbates the development of cerebral ischemia. Neuroscience 2015;310:674–85. https://doi.org/10.1016/j.neuroscience.2015.10.005. Epub 2015/10/11PubMed PMID: 26454021.

[23] Elfeber K, Stumpel F, Gorboulev V, Mattig S, Deussen A, Kaissling B, et al. Na(+)-D-glucose cotransporter in muscle capillaries increases glucose permeability. Biochem Biophys Res Commun 2004;314(2):301–5. https://doi.org/10.1016/j.bbrc.2003.12.090. Epub 2004/01/22PubMed PMID: 14733905.

[24] Yamazaki Y, Harada S, Wada T, Hagiwara T, Yoshida S, Tokuyama S. Sodium influx through cerebral sodium-glucose transporter type 1 exacerbates the development of cerebral ischemic neuronal damage. Eur J Pharmacol 2017;799:103–10. https://doi.org/10.1016/j.ejphar.2017.02.007. Epub 2017/02/09PubMed PMID: 28174043.

[25] Hirayama BA, Loo DD, Diez-Sampedro A, Leung DW, Meinild AK, Lai-Bing M, et al. Sodium-dependent reorganization of the sugar-binding site of SGLT1. Biochemistry 2007;46(46):13391–406. https://doi.org/10.1021/bi701562k. Epub 2007/10/27PubMed PMID: 17960916.

[26] Wright EM, Loo DD, Hirayama BA. Biology of human sodium glucose transporters. Physiol Rev 2011;91(2):733–94. https://doi.org/10.1152/physrev.00055.2009. Epub 2011/04/30PubMed PMID: 21527736.

[27] Jin S, Jeon JH, Lee S, Kang WY, Seong SJ, Yoon YR, et al. Detection of 13 ginsenosides (Rb1, Rb2, rc, Rd, Re, Rf, Rg1, Rg3, Rh2, F1, compound K, 20(S)-Protopanaxadiol, and 20(S)-Protopanaxatriol) in human plasma and application of the analytical method to human pharmacokinetic studies following two week-repeated administration of red ginseng extract. Molecules 2019;24(14). https://doi.org/10.3390/molecules24142618. Epub 2019/07/22PubMed PMID: 31323835; PubMed Central PMCID: PMCPMC6680484.

[28] Choi MK, Jin S, Jeon JH, Kang WY, Seong SJ, Yoon YR, et al. Tolerability and pharmacokinetics of ginsenosides Rb1, Rb2, Rc, Rd, and compound K after single or multiple administration of red ginseng extract in human beings. J Ginseng Res 2020;44(2):229–37. https://doi.org/10.1016/j.jgr.2018.10.006. Epub 2020/03/10PubMed PMID: 32148404; PubMed Central PMCID: PMCPMC7031742.

[29] Jeon J-H, Lee J, Choi M-K, Song I-S. Pharmacokinetics of ginsenosides following repeated oral administration of red ginseng extract significantly differ between species of experimental animals. Arch Pharm Res (Seoul) 2020;43(12):1335–46. https://doi.org/10.1007/s12272-020-01289-0.

[30] Bellut M, Papp L, Bieber M, Kraft P, Stoll G, Schuhmann MK. NLPR3 inflammasome inhibition alleviates hypoxic endothelial cell death in vitro and protects blood-brain barrier integrity in murine stroke. Cell Death Dis 2021;13(1):20. https://doi.org/10.1038/s41419-021-04379-z. Epub 2021/12/22PubMed PMID: 34930895; PubMed Central PMCID: PMCPMC8688414.

[31] Liu C, Wang J, Yang Y, Liu X, Zhu Y, Zou J, et al. Ginsenoside Rd ameliorates colitis by inducing p62-driven mitophagy-mediated NLRP3 inflammasome inactivation in mice. Biochem Pharmacol 2018;155:366–79. https://doi.org/10.1016/j.bcp.2018.07.010. Epub 2018/07/18PubMed PMID: 30012462.

[32] Greene C, Hanley N, Campbell M. Claudin-5: gatekeeper of neurological function. Fluids Barriers CNS 2019;16(1):3. https://doi.org/10.1186/s12987-019-0123-z. Epub 2019/01/30PubMed PMID: 30691500; PubMed Central PMCID: PMCPMC6350359.

[33] Phi LTH, Sari IN, Wijaya YT, Kim KS, Park K, Cho AE, et al. Ginsenoside Rd inhibits the metastasis of colorectal cancer via epidermal growth factor receptor signaling Axis. IUBMB Life 2019;71(5):601–10. https://doi.org/10.1002/iub.1984. Epub 2018/12/24PubMed PMID: 30576064.

[34] Liu X, Chen L, Liu M, Zhang H, Huang S, Xiong Y, et al. Ginsenoside Rb1 and Rd remarkably inhibited the hepatic uptake of ophiopogonin D in shenmai injection mediated by OATPs/oatps. Front Pharmacol 2018;9:957. https://doi.org/10.3389/fphar.2018.00957. Epub 2018/09/07PubMed PMID: 30186179; PubMed Central PMCID: PMCPMC6113708.

[35] Zhang C, Liu X, Xu H, Hu G, Zhang X, Xie Z, et al. Protopanaxadiol ginsenoside Rd protects against NMDA receptor-mediated excitotoxicity by attenuating calcineurin-regulated DAPK1 activity. Sci Rep 2020;10(1):8078. https://

doi.org/10.1038/s41598-020-64738-2. Epub 2020/05/18PubMed PMID: 32415270; PubMed Central PMCID: PMCPMC7228936.

[36] Rieg T, Vallon V. Development of SGLT1 and SGLT2 inhibitors. Diabetologia 2018;61(10):2079–86. https://doi.org/10.1007/s00125-018-4654-7. Epub 2018/08/23PubMed PMID: 30132033; PubMed Central PMCID: PMCPMC6124499.

[37] Koepsell H. The Na(+)-D-glucose cotransporters SGLT1 and SGLT2 are targets for the treatment of diabetes and cancer. Pharmacol Ther 2017;170:148–65. https://doi.org/10.1016/j.pharmthera.2016.10.017. Epub 2016/11/03PubMed PMID: 27773781.

[38] Tsai WH, Chuang SM, Liu SC, Lee CC, Chien MN, Leung CH, et al. Effects of SGLT2 inhibitors on stroke and its subtypes in patients with type 2 diabetes: a systematic review and meta-analysis. Sci Rep 2021;11(1):15364. https://doi.org/10.1038/s41598-021-94945-4. Epub 2021/07/30PubMed PMID: 34321571; PubMed Central PMCID: PMCPMC8319393.

[39] Pawlos A, Broncel M, Wozniak E, Gorzelak-Pabis P. Neuroprotective effect of SGLT2 inhibitors. Molecules 2021;26(23). https://doi.org/10.3390/molecules26237213. Epub 2021/12/11PubMed PMID: 34885795; PubMed Central PMCID: PMCPMC8659196.

[40] Vemula S, Roder KE, Yang T, Bhat GJ, Thekkumkara TJ, Abbruscato TJ. A functional role for sodium-dependent glucose transport across the blood-brain barrier during oxygen glucose deprivation. J Pharmacol Exp Therapeut 2009;328(2):487–95. https://doi.org/10.1124/jpet.108.146589. Epub 2008/11/05PubMed PMID: 18981287; PubMed Central PMCID: PMCPMC2630371.

[41] Munoz-Planillo R, Kuffa P, Martinez-Colon G, Smith BL, Rajendiran TM, Nunez G. K(+) efflux is the common trigger of NLRP3 inflammasome activation by bacterial toxins and particulate matter. Immunity 2013;38(6):1142–53. https://doi.org/10.1016/j.immuni.2013.05.016. Epub 2013/07/03PubMed PMID: 23809161; PubMed Central PMCID: PMCPMC3730833.